

COMPUTED TOMOGRAPHY OF CANINE ELBOW JOINTS AFFECTED BY PRIMARY AND CONCOMITANT FLEXOR ENTHESOPATHY

EVELIEN DE BAKKER, INGRID GIELEN, ANNEMIE VAN CAELENBERG, HENRI VAN BREE, BERNADETTE VAN RYSSEN

Flexor enthesopathy is an important differential diagnosis for elbow lameness in dogs. The disorder can be a primary cause of elbow lameness or concomitant with other elbow pathology. Since treatment differs for primary and concomitant forms of flexor enthesopathy, a noninvasive method for distinguishing between them is needed. In the current prospective study, computed tomographic (CT) examination was performed before and after IV injection of contrast in 17 dogs with primary flexor enthesopathy, 24 dogs with concomitant flexor enthesopathy, 13 dogs with elbow dysplasia, and seven normal dogs. Dogs were assigned to groups based on results of clinical examination and at least three other imaging modalities. Computed tomographic lesions consistent with flexor enthesopathy were found in all clinically affected joints with primary flexor enthesopathy and in 29 of the 30 clinically affected joints with concomitant flexor enthesopathy. Those lesions were not found in sound elbows or joints affected by elbow dysplasia. Flexor lesions detected in dogs with primary flexor enthesopathy were not significantly different from those detected in dogs with the concomitant form. Findings indicated that CT can be applied to detect flexor enthesopathy, but a distinction between the primary and concomitant forms was not always possible. Authors recommend the use of multiple diagnostic techniques for treatment planning in affected dogs. © 2013 American College of Veterinary Radiology.

Key words: computed tomography, diagnosis, dog, elbow, flexor enthesopathy.

Introduction

FLEXOR ENTHESOPATHY IS defined as an abnormality of the flexor muscles and their attachment to the medial humeral epicondyle.¹⁻⁴ It has been recently described as a differential diagnosis for elbow lameness in dogs.¹⁻⁴ Synonyms previously reported in the veterinary literature have included “united medial epicondyle.”⁵⁻¹⁰ Flexor enthesopathy can be considered primary when other underlying pathology of the elbow joint is absent. Flexor enthesopathy can be considered concomitant when it occurs in the presence of other elbow pathology such as medial coronoid disease and incongruity.^{2,3,6,9} The role of concomitant flexor enthesopathy lesions for dogs with elbow lameness remains unclear.⁴ A recent study described a prevalence of 6% for primary flexor enthesopathy and 34% for concomitant flexor enthesopathy in a group of lame dogs.² The current standard treatments for dogs with elbow lameness due to primary flexor enthesopathy include infiltration with

0.5–2 mg/kg bodyweight methylprednisolone acetate (Mod-erin 20 mg/ml, Pfizer A.H., Louvain la Neuve, Belgium) or surgical transection of the flexor muscles.^{1,3,11} The current standard treatment for dogs with elbow lameness due to concomitant flexor enthesopathy is surgical removal of the medial coronoid process fragment and/or cartilage flap and no treatment of the flexor lesion.² Effective treatment planning therefore requires accurate diagnosis of flexor enthesopathy and distinction between the primary and concomitant forms. Since the clinical signs are often nonspecific, imaging of the lesions is necessary.¹⁻³

Radiography and ultrasonography are good initial screening methods for detecting flexor enthesopathy in dogs and characteristics have been previously described.^{4,12} However, for some cases with confirmed flexor enthesopathy, both radiography and ultrasonography were unable to detect flexor lesions.^{4,12} In addition, both techniques were unable to distinguish primary flexor enthesopathy from the concomitant form.^{4,12}

Computed tomography (CT) is a noninvasive imaging technique that creates sectional images of anatomic structures.¹³ It has a high diagnostic accuracy and sensitivity for detection of bony lesions in elbow joints.¹⁴⁻¹⁷ Because CT produces sectional images of the elbow joint, it eliminates the problems of superimposition associated with conventional radiology.¹⁵ A recent clinical study concluded that CT was a valuable technique in the diagnosis of flexor

From the Department of Medical Imaging and Small Animal Orthopaedics (De Bakker) and Department of Medical Imaging, Veterinary Faculty, Ghent University, Merelbeke, Belgium (Gielen, van Bree, Van Ryssen, Van Caelenberg).

This study was funded by BOF grant 01D31908.

Address correspondence and reprint requests to Evelien de Bakker, Department of Medical Imaging and Small Animal Orthopaedics, Ghent University, Salisburylaan 133, Merelbeke 9820, Belgium. E-mail: Evelien.debakker@ugent.be

Received July 6, 2012; accepted for publication June 10, 2013.
doi: 10.1111/vru.12091

Vet Radiol Ultrasound, Vol. 55, No. 1, 2014, pp 45–55.

TABLE 1. Breed Distribution Within the Four Groups of Elbow Joints

Breed	Total dogs	Primary flexor enthesopathy (Joints)	Concomitant flexor enthesopathy (Joints)	Elbow dysplasia (Joints)	Normal (Joints)
Labrador Retriever	12	4	10	8	1
Great Swiss Mountain dog	5	7	1	0	1
Bernese Mountain dog	3	0	4	1	0
Rottweiler	5	5	4	0	1
Golden Retriever	5	2	4	2	2
Mixed Breed	3	4	2	0	0
Swiss Shepherd dog	1	0	1	0	0
Border Collie	1	2	0	0	0
French Bull dog	1	0	0	0	2
Newfoundlander	5	3	5	0	0
Saint Bernard dog	1	0	1	1	0
Dutch Partridge dog	1	2	0	0	0
Bouvier	1	0	2	0	0
Bullmastiff	1	0	2	0	0
Shepherd dog	1	0	0	2	0
Appenzeller	1	0	0	2	0
English Cocker Spaniel	1	0	0	2	0
Fox Hound	2	0	0	0	4
Total joints	50	29	36	18	11

enthesopathy in dogs.⁴ However, a detailed analysis of specific CT findings for primary versus concomitant forms of flexor enthesopathy was not performed. The addition of IV contrast with CT could also be a useful method for evaluating flexor enthesopathy lesions in dogs, since tendon injury and repair often cause new vessel formation and increased vascular permeability.^{18,19} The main disadvantages of CT are exposure to ionizing radiation and the need for general anesthesia.²⁰

The aims of the current study were to describe plain and IV contrast-enhanced CT characteristics of the flexor muscles and their attachment to the medial epicondyle in elbows diagnosed with flexor enthesopathy, and determine whether CT could be used to distinguish primary vs. concomitant forms of flexor enthesopathy in dogs. It was hypothesized that (1) CT would be a sensitive technique for detecting flexor enthesopathy; and (2) CT characteristics would differ between the two forms of flexor enthesopathy.

Materials and Methods

Dogs

Fifty dogs ($n = 50$) were prospectively investigated (Table 1). All of these dogs had also been used in previously published studies.¹² All dogs underwent a complete CT examination and received additional radiographic ($n = 50$), ultrasonographic ($n = 48$), scintigraphic (HisPECT)

($n = 45$), magnetic resonance imaging (MRI) ($n = 49$) and arthroscopic ($n = 50$) examinations. The prospective study was conducted in accordance with the guidelines of the Animal Care Committee of the Ghent University. The elbow joints of the 50 dogs were divided in four groups based on findings from at least three different imaging modalities. For 11 dogs, both elbow joints were assigned to different groups. Because of technical failures, six joints were excluded from the study.

Group 1 (primary flexor enthesopathy) consisted of 29 joints of 17 client-owned dogs with a mean age of 56.4 months (range 7–92 months). Eleven dogs were male, six were female. Dogs were included in this group when at least 3 of the 6 applied imaging modalities demonstrated lesions compatible with flexor enthesopathy and no other elbow lesions were detected.^{3,4} Radiographic signs of flexor enthesopathy were defined as an irregular outline of the medial epicondyle, bone spur(s), and/or a calcified body. Ultrasonographic signs were an abnormal fiber structure, abnormal attachment, irregular outline of the medial epicondyle, presence of a calcified body, and/or outward bowing of the flexor tendon. Scintigraphic signs were increased tracer uptake in the area of the medial humeral epicondyle. Magnetic resonance imaging signs were an irregular, sclerotic medial epicondyle, and thickened flexor muscles with contrast uptake and/or a calcified body. Arthroscopic signs were ruptured fibers at the insertion, thickened remnants, fibrillation, local synovitis, and local cartilage erosion.^{3,4} The absence of other elbow disorders such as medial coronoid process disease, osteochondritis dissecans, ununited anconeal process, and elbow incongruity was based on findings from both CT and arthroscopy. Seven elbow joints from dogs with no signs of elbow pain or lameness and with flexor enthesopathy lesions were considered subclinically affected and also included in this group.

Group 2 (concomitant flexor enthesopathy) consisted of 36 elbow joints from 24 client-owned dogs with a mean age of 50.4 months (range 7–104.4 months). Seventeen dogs were male and seven dogs were female. Dogs were included in this group when flexor lesions were demonstrated with at least three diagnostic imaging modalities (using the same criteria as those used for Group 1) and the additional presence of medial coronoid disease ($n = 29$), osteochondritis dissecans ($n = 3$) and medial coronoid disease + osteochondritis dissecans ($n = 4$) was detected using CT and arthroscopy.^{3,4} Eight of the joints included in this group had been treated arthroscopically for medial coronoid disease several years (1–6 years) before. Six joints from dogs with no signs of elbow pain or lameness were considered subclinically affected and also included in this group.

Group 3 (elbow dysplasia) consisted of 18 elbow joints from 13 client-owned dogs presenting with thoracic limb lameness with a mean age of 34.8 months (range 10–126 months). Eight dogs were male and five were female. For

all dogs included in this group, flexor enthesopathy was excluded based on the absence of flexor enthesopathy lesions in at least three other imaging modalities and the presence of medial coronoid process disease ($n = 18$) was confirmed based on CT and arthroscopy.

Group 4 (sound joints) consisted of two laboratory-owned and five client-owned dogs. The mean age was 64.8 months (range 19–126 months). This group consisted of five male dogs and two female dogs. For this group, 11 elbow joints were included in analysis based on absence of flexor enthesopathy and elbow dysplasia lesions using radiography, ultrasonography, scintigraphy, MRI, or arthroscopy.

CT Examination and Measurements

A four-slice helical CT device (GE Lightspeed QX/I; General Electric Co., Milwaukee, MI) was used for all scans. Prior to CT, dogs were sedated using acepromazine (0.01 mg/kg, IV) (Placivet®; Codifar, Wommelgem, Belgium) with medetomidine (28 µg/kg, IV) (Domitor, Pfizer Animal Health, Brussels) and then anesthetized with propofol (6 mg/kg, IV). After intubation, anesthesia was maintained with isoflurane in oxygen. Dogs were positioned on the scanning table in left lateral recumbency with both elbow joints parallel and extended cranially in order to scan both elbow joints simultaneously.¹⁷ The head of the dogs was pulled back to the lateral side to avoid artifacts.¹⁷ A wedge was positioned between the elbow joints in order to make them parallel to each other. A lateral scout view was performed to confirm correct positioning. Acquisition variables were 120 kV and 140 mA with a display field of view of 21 cm. A matrix size of 512 × 512, beam pitch of 0.75, slice pitch of 3 (HQ), and tube rotation time of 1 s were used. Transverse CT slices, in bone and soft tissue algorithm, of 1.25-mm thickness with an overlap of 0.6 mm were obtained from the proximal part of the ulna to 3 cm distal to the radial head, parallel to the humeroradial joint space. Immediately after this first scanning session, 2 ml/kg of 62.24 g iopromid (Ultravist 300; N.V. Shering S.A., Berlin, Germany) of contrast was injected intravenously by hand at a flow rate of 1 ml/s and contiguous slices in soft tissue algorithm were repeated. No pressure injector was used. The DICOM studies were retrieved and analyzed on a computer workstation using image analysis software (Merge Efilm, Merge eMed, Milwaukee, WI). Images of all elbow joints were evaluated in bone and soft tissue window with window width and level adjusted as needed. Two-dimensional, sagittal, and dorsal planar images were made with an image reconstruction interval of 0.6 mm. Findings for each elbow were recorded based on a consensus between a board-certified ECVDI diplomate (HvB) and the clinical head of the CT/MRI unit with 20 years experience (IG). Both assessors were unaware of the findings from other modalities and the final diagnosis at the

TABLE 2. Osteoarthritis Grading Scheme used for CT¹⁵

Osteoarthritis grade	Definition
0 (absent)	No osteophytes present
1 (mild)	Osteophytes <2 mm present
2 (moderate)	Osteophytes 2–5 mm present
3 (severe)	Osteophytes >5 mm present

time of image interpretation. The following bony and soft tissue parameters were recorded for each elbow: appearance of the medial humeral epicondyle (irregular delineation, sclerotic cortex, thickened cortex); presence/appearance of a calcified body (length (<3 mm, 3–mm, >5 mm), width (≤3 mm, >3 mm), close to medial epicondyle (<5 mm), and remote from medial epicondyle (≥5 mm)); thickening of the flexor muscles and contrast enhancement of the flexor muscles. Irregular and thickened medial epicondyle cortex characteristics were defined based on the periosteal margin of the medial epicondyle at the level of the flexor enthesis, while sclerosis was defined based on the subchondral margin of the medial epicondyle at the level of the flexor enthesis.

Thickening and contrast enhancement of the flexor muscles were based on comparison to normal elbow joints. Thickening of the flexor muscles was characterized by enlargement of the muscle belly and loss of fat density surrounding the flexor muscles. Contrast enhancement was calculated by measuring the Hounsfield units (HU) within a region of interest and comparing pre and postcontrast CT studies. Enhancement was determined as the difference in value between both density measurements. A difference of 10 HU was considered as the lower limit to be regarded as positive for increased enhancement.

In addition, the medial coronoid process was evaluated and the presence of lesions recorded (fragment, fissure, sclerosis, osteophytosis, demineralized tip). The medial aspect of the humeral condyle was inspected for the presence of osteochondritis dissecans lesions or an irregular delineation (kissing lesions). The presence of osteoarthritis was determined using a previously described four-point ordinal grading scheme (Table 2).¹⁵

Statistical Analysis

Statistical analyses were selected and performed by a statistical consultant and the first author (EdB). A Fisher's exact test was used to compare the frequencies of the different flexor enthesopathy parameters between dogs affected by primary flexor enthesopathy and dogs affected by concomitant flexor enthesopathy. A Mann–Whitney test was used to compare the flexor enthesopathy features between clinically and subclinically affected joints within each flexor enthesopathy group (SPSS statistics; IBM:

TABLE 3. Flexor lesions Seen in CT Scans of Clinically and Subclinically Affected Joints with Primary Flexor Enthesopathy and Concomitant Flexor Enthesopathy

CT Flexor lesion		Primary flexor enthesopathy		Concomitant flexor enthesopathy		P-value [†]
		Clinical (n = 22)*	Subclinical (n = 7)*	Clinical (n = 30)*	Subclinical (n = 6)*	
Medial Epicondyle	Irregular	18	2	26	1	0.78
	Sclerotic cortex	20	5	28	1	0.74
	Thickened cortex	20	5	28	0	0.52
Flexor muscle	Thickened	21	6	27	2	0.17
	Contrast enhancement	22	5	27	2	0.17
	Total	17	2	20	0	0.45
Calcified body	Length					
	<3 mm	5	1	7	0	1.00
	3–5 mm	5	0	8	0	0.76
	>5 mm	7	1	5	0	0.22
	Width					
	≤3 mm	11	1	15	0	1.00
	>3 mm	6	1	5	0	0.35
Location						
Close	5	0	12	0	0.17	
Remote	12	2	8	0	0.04	

*n = number of joints.

[†]P-value = probability.

Armonk, NY). Significance for all tests was set at a value of $P < 0.05$.

Results

Computed tomographic abnormalities of the medial humeral epicondyle and the attaching flexor muscles were found in all clinically affected joints with primary flexor enthesopathy and in 97% of the clinically affected joints with concomitant flexor enthesopathy. Computed tomography demonstrated flexor pathology in all subclinically affected joints of the primary group and in 3 of the 6 subclinically affected joints of the concomitant group. Abnormalities of the flexor muscles and their attachment to the medial humeral epicondyle were not found in sound elbow joints or those affected by elbow dysplasia.

Appearance of the Medial Humeral Epicondyle

An irregular outline of the medial humeral epicondyle was seen in 69% of the joints with primary and in 75% of the joints affected by concomitant flexor enthesopathy (P -value 0.78; Table 3; Figs. 1–3). Sclerosis of the medial epicondyle was seen in 86% of the joints with primary and 81% of the joints affected by concomitant flexor enthesopathy (P -value 0.74; Table 3; Figs. 1–3). A thickened cortex was present in 86% of the joints with primary and 78% of the joints with concomitant flexor enthesopathy (P -value 0.52; Table 3; Figs. 1–3). A combination of all three abnormalities of the medial epicondyle was seen in 69% of joints with primary and 67% of joints with concomitant flexor enthesopathy (Figs. 1–3). No statistically significant differences were found in the appearance of the medial humeral epi-

condyle between clinically and subclinically affected joints in both flexor enthesopathy groups (P -value primary 0.78, P -value concomitant 0.63).

Thickening of the Flexor Muscles

Thickening of the flexor muscles was seen in 93% of the joints with primary flexor enthesopathy and 81% of the joints with concomitant flexor enthesopathy (P -value 0.17; Table 3; Figs. 1 and 3). A statistically significant difference in thickening was found between clinically and subclinically affected joints in the concomitant flexor enthesopathy group (P -value 0.04). No significant difference in thickening was found between clinically and subclinically affected joints in the primary flexor enthesopathy group (P -value 0.64).

Presence of a Calcified Body

More than half of the joints of both flexor enthesopathy groups showed a calcified body on CT: 65.5% of the joints with primary and in 55.5% of the joints with concomitant flexor enthesopathy (P -value 0.45; Figs. 1–3). The only group of joints where no calcification was found was the subclinically affected joints of the concomitant flexor enthesopathy group (Table 3). No differences were found in length of the calcified body between flexor enthesopathy groups. The width was mostly medium (1–3 mm) in both groups. A significantly higher number of joints with primary flexor enthesopathy had a calcified body located remote to the medial humeral epicondyle (P -value 0.04; Table 3). In a minority of joints of both flexor enthesopathy groups multiple calcifications were noticed. A statistically

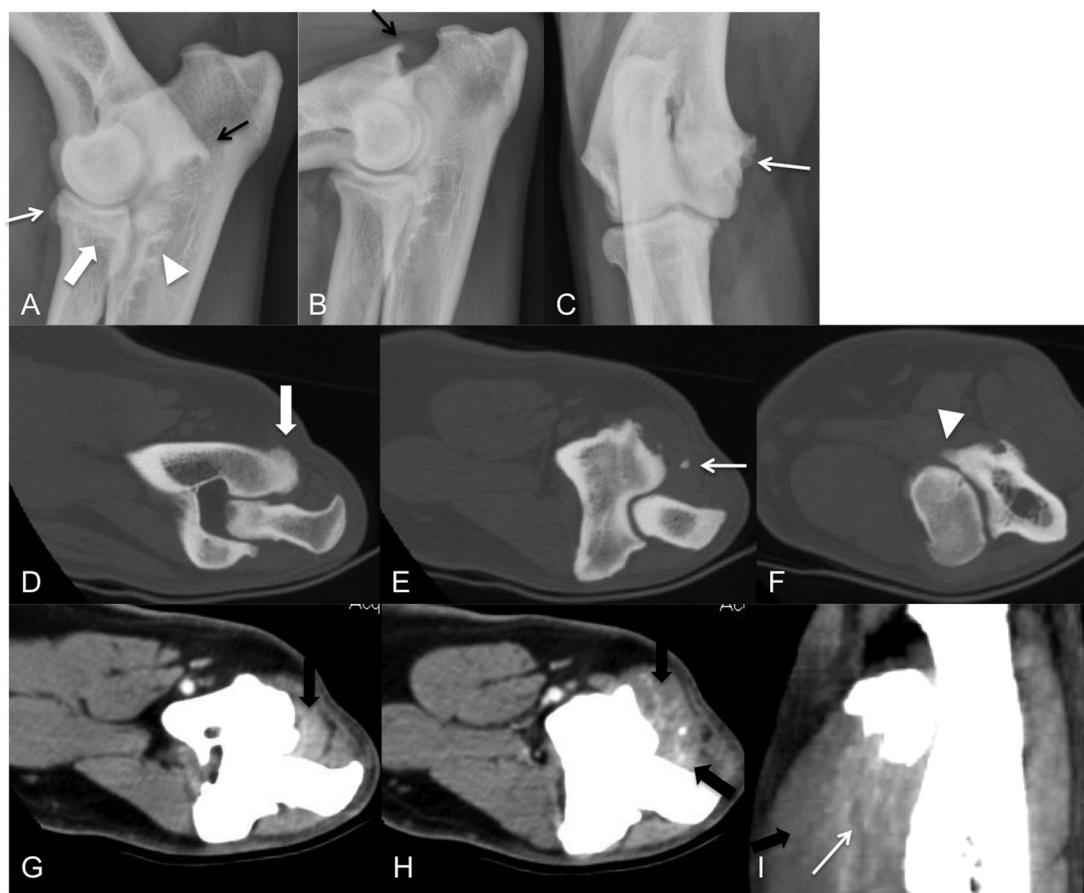


FIG. 1. Computed tomography images of the left elbow joint from a 4.5-year-old female Rottweiler with primary flexor enthesopathy. (A–C) Lateromedial extended (A), flexed (B) and 15° oblique craniolateral–caudomedial (C) radiographic images showing a clear spur (black arrow), mild osteoarthritis (small white arrow), an irregularly outlined medial coronoid process (broad white arrow), and a mild, patchy sclerotic aspect (white arrowhead). On the transverse CT images in bone algorithm (D–F), an irregularly delineated medial humeral epicondyle with a sclerotic and thickened cortex is visible (broad white arrow) with a small calcified body located close to the medial humeral epicondyle within thickened flexor muscles (small white arrow). The medial coronoid process shows hypo-attenuating new bone formation at the tip of the medial coronoid process representing an osteophyte (white arrowhead). Transverse CT images in soft tissue algorithm before (G) and after (H) IV injection of contrast demonstrate thickening of the flexor muscles with heterogeneous contrast enhancement (black arrows). The reconstructed image in dorsal plane after IV contrast (I) shows thickening of the flexor muscles (black arrow) and contrast enhancement within the flexor muscles (white arrow).

significant difference in length, width, and location of a calcified body was found between clinically and subclinically affected joints of both flexor enthesopathy groups (P -value 0.04).

Contrast Enhancement by Flexor Muscles

Ninety-three percent of the joints with primary flexor enthesopathy and 81% of the joints with concomitant flexor enthesopathy showed increased contrast enhancement in flexor soft tissues (P -value 0.17; Table 3). Increased enhancement was also a frequent finding in subclinically affected joints from the primary group (Table 3). A significantly higher contrast enhancement was found in joints with primary flexor enthesopathy (mean difference in contrast enhancement between pre and post contrast CT: 42 HU) compared to joints with concomitant flexor enthe-

sopathy (mean difference in contrast enhancement between pre and post contrast CT: 23 HU) (P -value 0.0001). Enhancement was visible within and around the flexor muscles (Figs. 1–3). Thickening without contrast enhancement was seen in one subclinically affected joint with primary flexor enthesopathy and in one clinically and one subclinically affected joint with concomitant flexor enthesopathy. No statistically significant differences in contrast enhancement were found between clinically and subclinically affected joints in both flexor enthesopathy groups (P -value primary 0.92, P -value concomitant 0.54).

Association between Flexor Abnormalities and Gradation of Osteoarthritis

Calcified bodies were often seen in combination with severe (grade 3) osteoarthritis in both flexor enthesopathy groups (Table 4). Other abnormalities of the medial



FIG. 2. Computed tomographic images of the right elbow joint from a 5.2-year-old male Dutch partridge dog with primary flexor enthesopathy. Radiographic images (lateromedial extended (A), lateromedial flexed (B), and 15° oblique craniolateral-caudomedial (C) projections) show a spur (small white arrow) and a medium and large calcified body close to the medial humeral epicondyle (small black arrows). The medial coronoid process is unclearly delineated (broad black arrow) with a mild amount of subtrochlear sclerosis (black arrowhead) and moderate osteoarthritis (broad white arrow). The transverse CT image in bone algorithm at the level of the humeral epicondyles (D) shows moderate osteoarthritis (small white arrows) and an irregular delineation of the caudal aspect of the medial humeral epicondyle with a sclerotic and thickened cortex (broad black arrow). A large calcified body is visible close to the medial humeral epicondyle (broad white arrow). The joint space between the humerus and ulna is widened, suggesting incongruity (small black arrow). The transverse CT image in bone algorithm at the level of the medial coronoid process (E) demonstrates an osteophyte (black arrow). A large calcified body within the flexor muscles is visible (white arrow). The transverse CT image in soft tissue algorithm after IV contrast at the level of the humeral epicondyles (F) shows contrast enhancement within the flexor muscles and around the calcified body (black circle). On the three-dimensional reconstructed dorsal image (G), the large calcified body is visible just below the medial humeral epicondyle (white arrow). The dorsal reconstruction after IV contrast (H) demonstrates contrast enhancement within the flexor muscles and around the calcified body (black arrow; white arrow pointing at the calcified body).

humeral epicondyle and the flexor muscles were also present in combination with lower grades of osteoarthritis (grade 0 and grade 1), which was more prominent and statistically significant in the primary group (P -value 0.002; Table 4).

Presence of other Elbow Disorders

Abnormalities of the medial coronoid process were seen in all joints with elbow dysplasia and in all but one of the joints affected by concomitant flexor enthesopathy

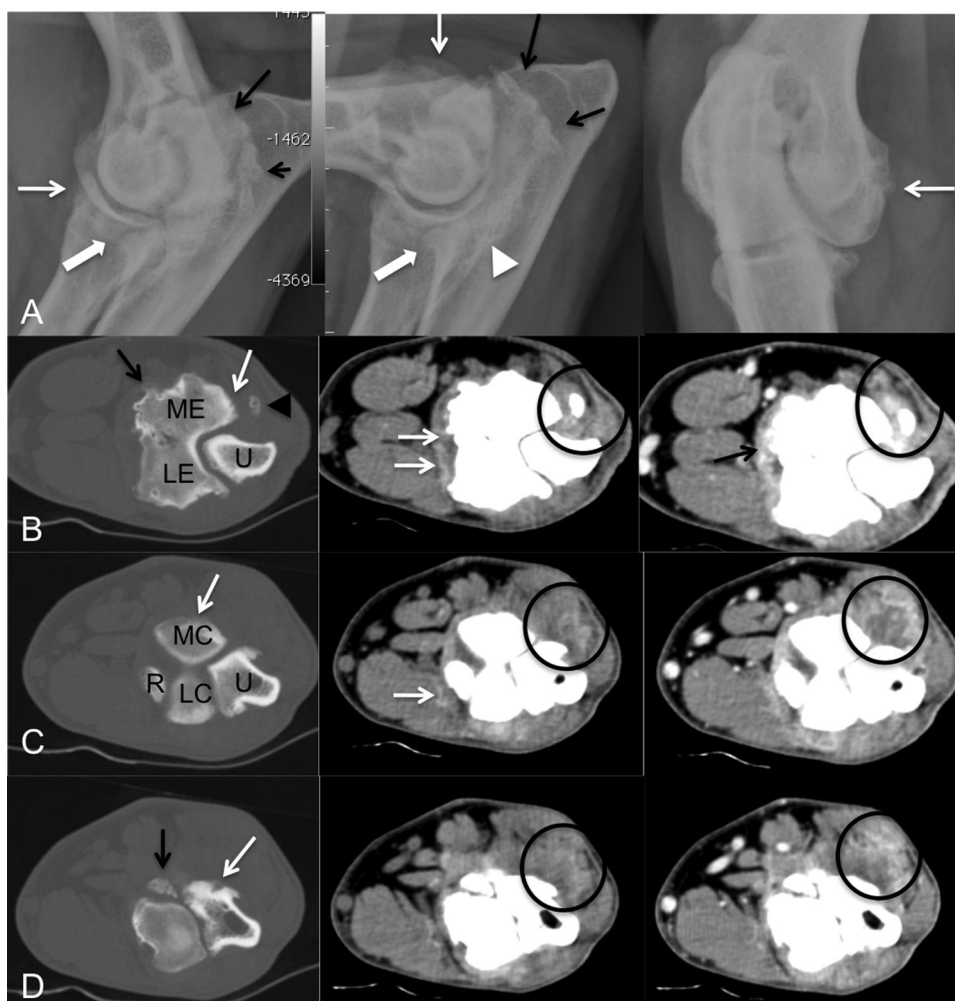


FIG. 3. Computed tomographic images of the left elbow joint from a 3.7-year-old male Bernese mountain dog with concomitant flexor enthesopathy. Row A: Radiographic images (lateromedial extended, flexed and 15° oblique craniolateral-caudomedial projections) demonstrating a medium and large calcified body near the medial humeral epicondyle (black arrows). The medial coronoid process is fragmented (broad white arrow), with severe osteoarthritis (small white arrow) and subtrocchlear sclerosis (white arrowhead). Row B–D: Transverse CT images in bone algorithm (left column), in soft tissue algorithm (middle column) and in soft tissue algorithm after IV contrast (right column) at different levels of the elbow joint. Row B is at the level of the humeral epicondyles, showing new bone formation (black arrow) and an irregular delineation with a thickened and sclerotic cortex (white arrow). A small calcified body is visible at the level of the flexor muscles (black arrowhead). The soft tissue algorithm shows a hyperattenuating joint capsule (middle column, white arrows) and a calcified body within the flexor muscles (middle column, black circle). There is contrast enhancement of the joint capsule (right column, black arrow), within the flexor muscles and around the calcified body (right column, black circle). Row C is at the level of the distal humeral condyles with new bone formation (white arrow). A hyperattenuating joint capsule (middle column, white arrow) and thickened, more hyperattenuating (presumably due to fibrosis or mini mineralizations) flexor muscles (middle column, black circle) are visible. Contrast enhancement of the flexor muscles is visible (right column, black circle). MC = medial humeral condyle, LC = lateral humeral condyle, R = radius, U = ulna. Row D is at the level of the medial coronoid process showing a large, displaced fragment (left column, black arrow) and osteophytes (left column, white arrow). A thickened, hyperattenuating appearance of the flexor muscles is visible (middle column, black circle) with contrast enhancement (right column, black circle).

(Table 5; Fig. 3). In 55% of the joints with primary flexor enthesopathy, osteophytes on the medial coronoid process were found (Figs. 1 and 2). Osteochondritis dissecans without medial coronoid process disease was seen in three joints affected by concomitant flexor enthesopathy (22%). Kissing lesions affecting the medial humeral condyle were found in 11% of the joints affected by elbow dysplasia, 28% of joints with concomitant flexor enthesopathy, and 6% of joints with primary flexor enthesopathy (Table 5; Fig. 4).

Discussion

In the present study, CT demonstrated flexor pathology in all clinically affected joints with primary flexor enthesopathy and in 97% of the clinically affected joints with concomitant flexor pathology. This suggests that CT can be considered a sensitive technique for detecting flexor enthesopathy in dogs. In humans with a similar condition (medial epicondylitis or Golfer's elbow), the diagnostic work-up mostly includes radiography, ultrasonography and

TABLE 4. Correlation Between Osteoarthritis Grade and CT Flexor Lesions for Joints Affected by Primary Flexor Enthesopathy and Joints affected by Concomitant Flexor Enthesopathy

	Irregular, thickened, sclerotic epicondyle		Thickened flexor muscles with contrast		Calcified body	
	PFE (<i>n</i> = 25) [§]	CFE (<i>n</i> = 28) [§]	PFE (<i>n</i> = 27) [§]	CFE (<i>n</i> = 29) [§]	PFE (<i>n</i> = 19) [§]	CFE (<i>n</i> = 20) [§]
Grade 0	2	1	5	1	0	0
Grade 1	13	8	12	8	3	2
Grade 2	5	9	5	9	5	5
Grade 3	5	10	5	11	11	13

Gradation of osteoarthritis is based on a four-point ordinal grading scheme.¹⁵

§ PFE = primary flexor enthesopathy, CFE = concomitant flexor enthesopathy, *n* = number of elbow joints with each CT flexor lesion.

TABLE 5. Distribution of Osteoarthritis Grade, Appearance of the Medial Coronoid Process, Osteochondritis Dissecans and Longitudinal Sclerotic Stripes of the Medial Part of the Humeral Condyle for Elbows Affected by Primary Flexor Enthesopathy, Elbows Affected by Concomitant Flexor Enthesopathy, and Elbows Affected by Elbow Dysplasia

Pathology		PFE (<i>n</i> = 29) [§]	CFE (<i>n</i> = 36) [§]	ED (<i>n</i> = 18) [§]
Osteoarthritis	Grade 0	6	1	13
	Grade 1	13	13	3
	Grade 2	5	10	2
	Grade 3	5	12	0
MCP	Fragment	0	24	11
	Fissure	0	2	4
	Sclerosis	0	0	1
	Osteophytes	16	20	3
	Demineralised tip	0	3	0
OCD		0	3	0
MCD + OCD		0	5	0
Sclerotic stripes MHC		2	10	2

Gradation of osteoarthritis was based on a four-point ordinal grading scheme.¹⁵

§PFE = primary flexor enthesopathy, CFE = concomitant flexor enthesopathy, ED = elbow dysplasia, MCP = medial coronoid process, OCD = osteochondritis dissecans, MHC = medial part of the humeral condyle, *n* = number of elbow joints.

MRI.^{21,22} In dogs, recent studies on the diagnosis of flexor enthesopathy demonstrated an inability of both radiography and ultrasonography to detect and distinguish the two forms of flexor enthesopathy.^{4,12}

The mean age of the dogs with primary flexor enthesopathy in the current study was 4.7 years, which is comparable to previous reports on medial epicondylar lesions.^{3,6,9} Concomitant flexor enthesopathy was seen in dogs with a mean age of 4.2 years. Since many joints were chronically affected or had been treated arthroscopically several years before, the mean age was higher than would be expected for medial coronoid disease which was the main concomitant disorder.²³ The mean age of dogs affected by elbow dysplasia was 2.9 years, which is consistent with literature on elbow dysplasia describing both young and older dogs.^{24–27} The higher mean age of dogs with normal elbow joints compared to both flexor enthesopathy groups in the current study is considered irrelevant since no pathology was present. In both flexor enthesopathy groups, male dogs were more frequently affected than female dogs. This find-

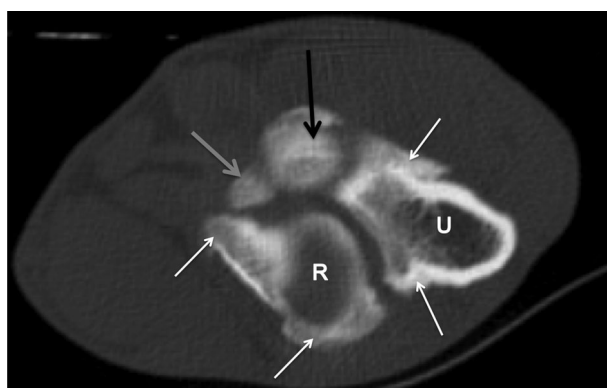


FIG. 4. Transverse CT image in bone algorithm at the level of the joint space demonstrating a sclerotic stripe or kissing lesion of the medial part of the humeral condyle (black arrow). Osteoarthritic changes are visible (white arrows) at the level of the ulna and the radial head. There is a fragmented coronoid process; the large fragment is displaced cranially (gray arrow). R: radius; U: ulna.

ing suggests a gender predilection, which is consistent with literature.^{6,9,23} Primary and concomitant flexor enthesopathy were mainly seen in medium- and large-breed dogs. The Great Swiss Mountain dog was the most represented breed in the primary flexor enthesopathy group (24%), followed by Rottweiler (17%) and Labrador Retriever (14%). This higher prevalence in the Great Swiss Mountain Dog was remarkable, since it is considered a less common breed. Both normal and elbow dysplasia groups were mostly represented by medium- and large-breed dogs. However, some small-breed dogs (French Bulldog, Appenzeller and English Cocker Spaniel) were included in both control groups, which is justified since medial coronoid disease has also been described in small-breed dogs.²⁶

In eight joints of the concomitant group (which had previously been treated for medial coronoid disease and/or osteochondritis dissecans) no signs of flexor enthesopathy were found at the time of initial treatment. Apparently, some joints affected by medial coronoid disease and/or osteochondritis dissecans may develop concomitant flexor enthesopathy after arthroscopic treatment.⁴ Trauma caused by arthroscopic intervention or increased inflammation induced by the lesions or the arthroscopic treatment may have caused the development of enthesopathy and local

myopathy. However, in the authors' experience, this is not routinely observed. An ongoing study on the long-term clinical and radiographic follow-up with special attention to this condition should clarify this evolution. In cases of recurrent lameness after initial treatment of medial coronoid disease it is unclear whether the relapse can be explained by the medial coronoid process problem or by the development of flexor enthesopathy.⁴

Bony changes at the flexor attachment to the medial epicondyle were easily diagnosed with CT. Frequent signs seen in both flexor enthesopathy groups were sclerosis and a thickened cortex of the medial humeral epicondyle. An irregular outline of the medial epicondyle was less frequently seen. No significant differences in bony changes were found between the two flexor enthesopathy groups. These changes at the medial epicondyle can be explained as a skeletal response to high tensile forces within a tendon, as is described in medial epicondylitis in man.²⁸ However, an irregular outline of the medial epicondyle has also been described as a sign of osteoarthritis and considered to be an expected finding in any joint affected by an elbow disorder, similar to the radiographic epicondylar changes.^{1-3,12} Indeed most elbows of both flexor enthesopathy groups in our study with an irregular outline of the medial epicondyle showed a moderate-to-severe grade of osteoarthritis. An irregular outline was absent in joints with elbow dysplasia, and most of these joints had no osteoarthritis. However, some joints of the primary and concomitant group showed an irregular outline without other bony changes suggestive for osteoarthritis. Therefore, this CT sign should not be exclusively considered as an early sign of osteoarthritis, but also regarded as a specific sign of flexor enthesopathy.

Both thickening of the flexor muscles and contrast enhancement were found in 93% of the joints with primary and 81% of the joints with concomitant flexor enthesopathy. The higher contrast enhancement in the primary flexor enthesopathy group may indicate that pathology was concentrated in that area. However, since contrast enhancement was also seen in both flexor groups it cannot be used as a distinctive parameter. Thickening of the flexor muscles can be explained by the presence of fibrous or granulation tissue between or within the flexor muscles, formed as a reparative response to microtrauma exerted on the flexor muscles.²⁹ An increase in contrast concentration within the flexor muscles can be explained by an increase of blood flow and vascular permeability of the tendon tissue, which is in turn part of the tendon injury and repair mechanism.¹⁹ A similar increase in contrast concentration was described in inflammatory and neoplastic tissue caused by an increase in perfusion and vascular permeability.¹⁸ Since the additional costs for contrast-enhanced CT are quite low and it only requires a few additional slices, we recommend this additional examination for the diagnostic work-up of any elbow suspected for lesions other than elbow dysplasia.

A calcified body was found in the majority of joints for both flexor enthesopathy groups, which is consistent with literature describing a calcified body as the most frequent sign of flexor enthesopathy.^{1,3,5,6,9,10,30,31} The presence of a calcified body can be considered part of the tendon degeneration process in tendinopathies.¹¹ In man, several stages of medial epicondylitis have been described. In the early stages, inflammatory or synovitic characteristics may be visible. In later stages, results of microtearing can be seen, characterized by tendon degeneration and often accompanied by the presence of calcified bodies.¹¹ Although the length of the calcified bodies in our study was mostly larger in the primary form this was not a significant difference. Also the width of the calcified body was not different between both groups. The only significant difference was the localization of the calcified body. In a significantly higher number of joints affected by primary flexor enthesopathy, the calcification was located further away from the medial humeral epicondyle than in concomitant flexor enthesopathy joints. However, this finding alone was insufficient to make a distinction between both forms of flexor enthesopathy. In nearly all cases of flexor enthesopathy a calcification was seen in combination with grade 2 or 3 osteoarthritis. Similar to medial epicondylitis in man, the presence of a calcified body presumably represents a later stage of the disorder, involving degenerative changes of the elbow joint.¹¹ In contrast, abnormalities of the medial humeral epicondyle and the flexor muscles were correlated with lower grades of osteoarthritis, especially in joints with primary flexor enthesopathy.

All seven subclinically affected joints of the primary flexor enthesopathy group and 3 of 6 subclinically affected joints of the concomitant flexor enthesopathy group demonstrated clear CT signs of flexor enthesopathy. Although there were some statistically significant differences in specific details, these features were not conclusive because they were also seen in the other groups at a lower frequency. The high number of subclinically affected joints detected with CT is consistent with a previous study of 200 elbows, which described medial epicondylar changes as coincidental findings.¹ However, three subclinically affected joints with concomitant flexor enthesopathy were not detected on CT or radiography. These joints were diagnosed with concomitant flexor enthesopathy based on additional ultrasonographic, scintigraphic, MRI, and arthroscopic examination. The absence of flexor pathology on both radiography and CT can be explained by the fact that, in the early stage, only the soft tissues are affected. The detection of pathology found with other diagnostic techniques does not necessarily have a clinical meaning, since this was mainly seen in subclinically affected joints.

Computed tomographic and arthroscopic findings were used as reference standards to confirm or exclude elbow dysplasia in this prospective study.¹⁵ In 55% of the joints

diagnosed with primary flexor enthesopathy, CT revealed osteophytes at the medial coronoid process. Based on the CT findings these joints could have been diagnosed with concomitant flexor enthesopathy, because of suspected medial coronoid lesions. However, arthroscopic examination of these joints excluded an abnormal appearance of the medial coronoid process. In all but one joint of the concomitant group, CT confirmed an abnormal appearance of the medial coronoid process. In this one joint, CT showed a normal medial coronoid process while arthroscopy demonstrated chondromalacia. This can be explained by the presence of cartilaginous lesions that are not detectable by CT.¹⁵ With CT, all cases of osteochondritis dissecans in the concomitant group were correctly diagnosed. Longitudinal sclerotic stripes of the medial part of the humeral condyle (kissing lesions) were a frequent finding in joints of the concomitant group with severe degrees of osteoarthritis. The presence of those sclerotic stripes reflects the severity of lesions in chronically affected joints with concomitant flexor enthesopathy. However, CT also demonstrated sclerotic stripes of the medial part of the humeral condyle in two joints diagnosed with primary flexor enthesopathy. These joints showed severe degenerative changes and the sclerotic stripes of the medial part of the humeral condyle

were considered part of the degenerative process. Since the enthesis (the attachment site of the flexor muscles at the medial humeral epicondyle) is often damaged in joints affected by flexor enthesopathy, the underlying synovial membrane may be consequently disrupted, involving the entire joint and resulting in degenerative changes.⁴

In conclusion, results of the current study supported our first hypothesis that CT can be considered a sensitive technique for the detection of flexor enthesopathy in clinically affected canine elbow joints. However, study results rejected our second hypothesis in that only minor significant differences in CT signs of flexor enthesopathy were identified and these were insufficient to make the difference between the primary and the concomitant form. Furthermore, discrete lesions of the medial coronoid process may be difficult to diagnose with CT, which makes an indirect distinction between the primary and concomitant form not always possible solely based on CT findings. This illustrates the need for multiple diagnostic modalities to differentiate between primary and concomitant forms of flexor enthesopathy.

ACKNOWLEDGMENTS

The authors wish to thank Professor J. DeWulf for his help with the statistical analysis.

REFERENCES

- de Bakker E, Samoy Y, Gielen I, Van Ryssen B. Medial humeral epicondylar lesions in the canine elbow. A review of the literature. *Vet Comp Orthop Traumatol* 2011;24:9–17.
- de Bakker E, Saunders J, Gielen I, van Bree H, Coppeters E, Van Ryssen B. Radiographic findings of the medial humeral epicondyle in 200 canine elbow joints. *Vet Comp Orthop Traumatol* 2012;25:359–365.
- Van Ryssen B, de Bakker E, Beauclin Y, et al. Primary flexor enthesopathy of the canine elbow: imaging and arthroscopic findings in eight dogs with discrete radiographic changes. *Vet Comp Orthop Traumatol* 2012;25:239–243.
- de Bakker E, Gielen I, Saunders JH, et al. Primary and concomitant flexor enthesopathy of the canine elbow. *Vet Comp Orthop Traumatol* 2013;26: [Epub ahead of print].
- Ljunggren G, Cawley AJ, Archibald J. The elbow dysplasias in the dog. *J Am Vet Med Assoc* 1966;148:887–891.
- Zontine WJ, Weitkamp RA, Lippincott CL. Redefined type of elbow dysplasia involving calcified flexor tendons attached to the medial humeral epicondyle in three dogs. *J Am Vet Med Assoc* 1989;194:1082–1085.
- Walker TM. A redefined type of elbow dysplasia in the dog—2 cases. *Can Vet J* 1998;39:573–575.
- Paster ER, Biery DN, Lawler DF, et al. Un-United Medial Epicondyle of the Humerus: Radiographic Prevalence and Association with Elbow Osteoarthritis in a Cohort of Labrador Retrievers. *Vet Surg* 2009;38:169–172.
- Meyer-Lindberg A, Heinen V, Hewicker-Trautwein M, Nolte I. Vorkommen und Behandlung von knöchernen Metaplasien in den am medialen Epikondylus des Humerus entspringenden Beugesehnen beim Hund. *Tierarztl Prax* 2004;32:276–285.
- Grondalen J, Braut T. Lameness in two young dogs caused by a calcified body in the joint capsule of the elbow. *J Small Anim Pract* 1976;17:681–684.
- Ciccotti MC, Schwartz MA, Ciccotti MG. Diagnosis and treatment of medial epicondylitis of the elbow. *Clin Sports Med* 2004;23:693–705, xi.
- de Bakker E, Saunders JH, van Bree H, Gielen I, Van Ryssen B. Radiographic features of primary and concomitant flexor enthesopathy in the canine elbow. *Vet Radiol Ultrasound* 2013;54:107–113.
- Tromblee TC, Jones JC, Bahr AM, Shires PK, Aref S. Effect of computed tomography display window and image plane on diagnostic certainty for characteristics of dysplastic elbow joints in dogs. *Am J Vet Res* 2007;68:858–871.
- Reichle JK, Park RD, Bahr AM. Computed tomographic findings of dogs with cubital joint lameness. *Vet Radiol Ultrasound* 2000;41:125–130.
- Moore AP, Benigni L, Lamb CR. Computed tomography versus arthroscopy for detection of canine elbow dysplasia lesions. *Vet Surg* 2008;37:390–398.
- Carpenter LG, Schwarz PD, Lowry JE, Park RD, Steyn PF. Comparison of radiologic imaging techniques for diagnosis of fragmented medial coronoid process of the cubital joint in dogs. *J Am Vet Med Assoc* 1993;203:78–83.
- De Rycke LM, Gielen IM, Van BH, Simoens PJ. Computed tomography of the elbow joint in clinically normal dogs. *Am J Vet Res* 2002;63:1400–1407.
- Puchalski SM, Galuppo LD, Drew CP, Wisner ER. Use of contrast-enhanced computed tomography to assess angiogenesis in deep digital flexor tendinopathy in a horse. *Vet Radiol Ultrasound* 2009;50:292–297.
- Sharma P. N. M. Tendon injury and tendinopathy: healing and repair. *J Bone Joint Surg* 2005;87:187–202.
- Cook CR, Cook JL. Diagnostic imaging of canine elbow dysplasia: a review. *Vet Surg* 2009;38:144–153.
- Park GY, Lee SM, Lee MY. Diagnostic value of ultrasonography for clinical medial epicondylitis. *Arch Phys Med Rehabil* 2008;89:738–742.
- Walz DM, Newman JS, Konin GP, Ross G. Epicondylitis: pathogenesis, imaging, and treatment. *Radiographics* 2010;30:167–184.
- Berzon JL, Quick CB. Fragmented coronoid process: anatomical, clinical and radiographic considerations with case analyses. *J Am Anim Hosp Assoc* 2006;16:241–251.

24. Vermote KA, Bergenhuyzen AL, Gielen I, van Bree H, Duchateau L, Van Ryssen B. Elbow lameness in dogs of six years and older. *Vet Comp Orthop Traumatol* 2010;23:43–50.
25. Olsson SE. The early diagnosis of fragmented coronoid process and osteochondrosis dissecans of the canine elbow joint. *J Am Anim Hosp Assoc* 1983;19:616–626.
26. Fitzpatrick N, Smith TJ, Evans RB. Radiographic and arthroscopic findings in the elbow joints of 263 dogs with medial coronoid disease. *Vet Surg* 2009;38:213–223.
27. Grondalen J. Arthrosis with special reference to the elbow joint of young rapidly growing dogs. I A review of the literature. *Nordisk Veterinaermedicin* 1979;31:62–68.
28. Rogers J, Shepstone L, Dieppe P. Bone formers: osteophyte and enthesophyte formation are positively associated. *Ann Rheum Dis* 1997;56:85–90.
29. Benjamin M, Toumi H, Ralphs JR, Bydder G, Best TM, Milz S. Where tendons and ligaments meet bone: attachment sites ('entheses') in relation to exercise and/or mechanical load. *J Anat* 2006;208:471–490.
30. Harasen G. The mysterious dysplastic elbow. *Can Vet J* 2003;44:673–674.
31. May C, Bennett D. Medial epicondylar spur associated with lameness in dogs. *J Small Anim Pract* 1988;29:797–803.